Journal of Power Sources 196 (2011) 6788–6793

Contents lists available at ScienceDirect

Journal of Power Sources

journal homepage: www.elsevier.com/locate/jpowsour

Microwave synthesis of novel high voltage (4.6 V) high capacity $LiCu_xCo_{1-x}O_{2\pm\delta}$ cathode material for lithium rechargeable cells

C. Nithya, R. Thirunakaran, A. Sivashanmugam, S. Gopukumar*

Central Electrochemical Research Institute (CSIR), Karaikudi 630 006, Tamil Nadu, India

ARTICLE INFO

Article history:
Received 26 July 2010
Received in revised form 7 October 2010
Accepted 18 October 2010
Available online 25 October 2010

Keywords:
Microwave method
Layered material
Charge/discharge studies

ABSTRACT

Layered $LiCu_xCo_{1-x}O_{2\pm\delta}$ $(0.0 \le x \le 0.3)$ has been synthesized using microwave method. This method possesses many advantages such as homogeneity of final product and shorter reaction time compared to other conventional methods. The structure and electrochemical properties of the synthesized materials are characterized through various methods such as XRD, SEM, FTIR, XPS and galvanostatic charge/discharge studies. The XRD patterns of $LiCu_xCo_{1-x}O_{2\pm\delta}$ confirm the formation of single-phase layered material. SEM images show that the particles are agglomerated and the average particle size decreases with increasing amount of copper. Electrochemical cycling studies are carried out between 2.7 and 4.6 V using 1 M $LiPF_6$ in 1:1 EC/DEC as electrolyte. The charge/discharge cycling studies of layered material with $LiCu_{0.2}Co_{0.8}O_{19}$ exhibit an average discharge capacity of ~150 mAh g^{-1} over the investigated 50 cycles.

1. Introduction

Lithium based transition metal oxides $LiMO_2$ (M = Ni, Co and Mn) have specific properties such as high energy density, long cycle life, good safety, constant discharging properties and wide range of working temperatures. Among these compounds, $LiCoO_2$ is still the most widely used cathode material in commercial lithium batteries and molten carbonate fuel cells [1,2]. It has α-$NaFeO_2$ layered structure, in which Li ions occupy the 3a sites, Co ions occupy the 3b sites and oxygen ions occupy the 6d sites [3]. The practical capacity of $LiCoO_2$ is limited to about 140 mAh g^{-1} i.e., half of theoretical capacity (273 mAh g^{-1}) because of the degradation of the crystal structure occurs due to the dislocation of lattice oxygen at high temperatures and overcharge to 4.2 V [4]. This structural instability results in restricted cycling performance. To reduce the influence of structural and stress effects on the electrochemical performance of $LiCoO_2$, substitution of Co for other transition metals such as Al, Zr, Ti, and Mg has been investigated [5–7]. However, these attempts failed to enhance the capacity and also to increase the structural stability of $LiCoO_2$ during cycling when charged to higher voltages i.e., above 4.3 V. Metal powders especially Cu or Ag have been found to mainly increase the capacity of the layered cathode materials [8–10]. Deepa et al. reported [11] that Cu dopant increases the stability of $LiCoO_2$ and Zou et al. [12] also found that $LiCu_{0.05}Co_{0.95}O_2$ synthesized via melt impregnation technique in an argon atmosphere cycled up to 4.5 V thereby demonstrating higher capacity and cycling stability. Lala et al. [13] found that Ga doped $LiCoO_2$ exhibits poor performance when Li is extracted at 4.7 V. Further investigations on the coating of $LiCoO_2$ with ceramic materials such as Al_2O_3, ZrO_2 (4.5 V) [14,15], La_2O_3 [16] (4.6 V) and nanocrystalline MgO [17] (4.7 V) are found to increase the capacity. Therefore, it is seen that no report is available on the cycling stability at 4.6 V of doped $LiCoO_2$ with either Cu or Al.

Several synthetic methods have been employed for the synthesis of transition metal oxides such as co-precipitation, hydrothermal method, combustion method and emulsion–drying method. These methods usually produce homogeneous electrode materials. However, high temperature calcination processes require longer heating times and with necessary intermediate grinding to obtain satisfactory crystallinity. Microwave irradiation to transition metal oxides usually results in faster heating of the compounds so that the desired final product can be obtained within very short time [18]. Recently, we have reported the synthesis of Mg doped $LiCoO_2$ [5] material irradiated by 50% microwave power followed by calcination at 850 °C. It is observed that 50% microwave power is not enough to obtain the required final product. Hence, in this paper, we report the synthesis of divalent substituted Cu^{2+} into the Co site in $LiCoO_2$ cathode material using microwave method only without further calcinations. Moreover, the synthesized material has been investigated for its electrochemical performance up to 4.6 V. Furthermore, the microwave synthesis is more advantageous from commercial and economic point of view than other methods and it is expected that Cu doping enhance the structural stability of the materials.

* Corresponding author. Tel.: +91 4565 227559; fax: +91 4565 227779.
E-mail address: deepika.41@rediffmail.com (S. Gopukumar).

0378-7753/$ – see front matter © 2010 Published by Elsevier B.V.
doi:10.1016/j.jpowsour.2010.10.053

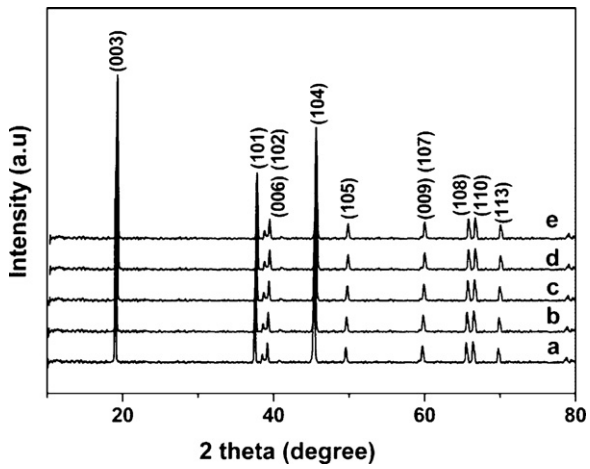

Fig. 1. XRD patterns of $LiCu_xCo_{1-x}O_{2\pm\delta}$ (a) $x = 0.00$, (b) $x = 0.05$, (c) $x = 0.10$, (d) $x = 0.20$ (e) $x = 0.30$ samples synthesized by microwave method.

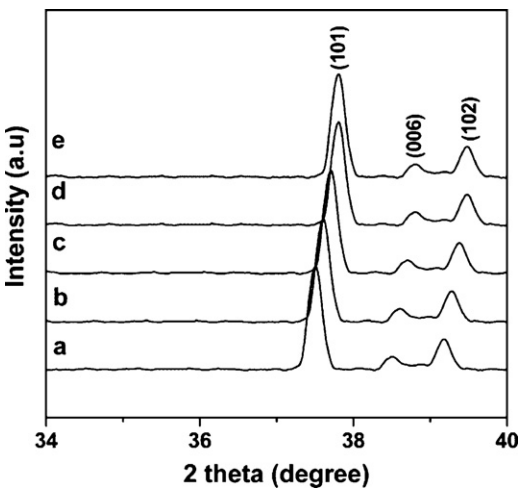

Fig. 2. Magnified XRD patterns of $LiCu_xCo_{1-x}O_{2\pm\delta}$ between 2θ values corresponding to 34–40° (a) $x = 0.00$, (b) $x = 0.05$, (c) $x = 0.10$, (d) $x = 0.20$ (e) $x = 0.30$.

2. Experimental

Stoichiometric amounts of anhydrous $LiNO_3$, $Co(NO_3)_2{\cdot}4H_2O$ containing with or without $Cu(NO_3)_2{\cdot}3H_2O$ were mixed thoroughly and dissolved in triple distilled water. The resulting metal ion solution was concentrated by stirring continuously under slightly warmed condition (70 °C). The above concentrated solution was transferred to a china dish and placed at the centre of a rotating plate of microwave oven (Kenstar, India 2450 MHz, 800 W). The solution was irradiated at 100% power for 25 min. During the reaction, the chemical constituents were rapidly heated and a red glow was seen inside the china dish throughout the reaction. After completion of the reaction, the product was dried well in an air

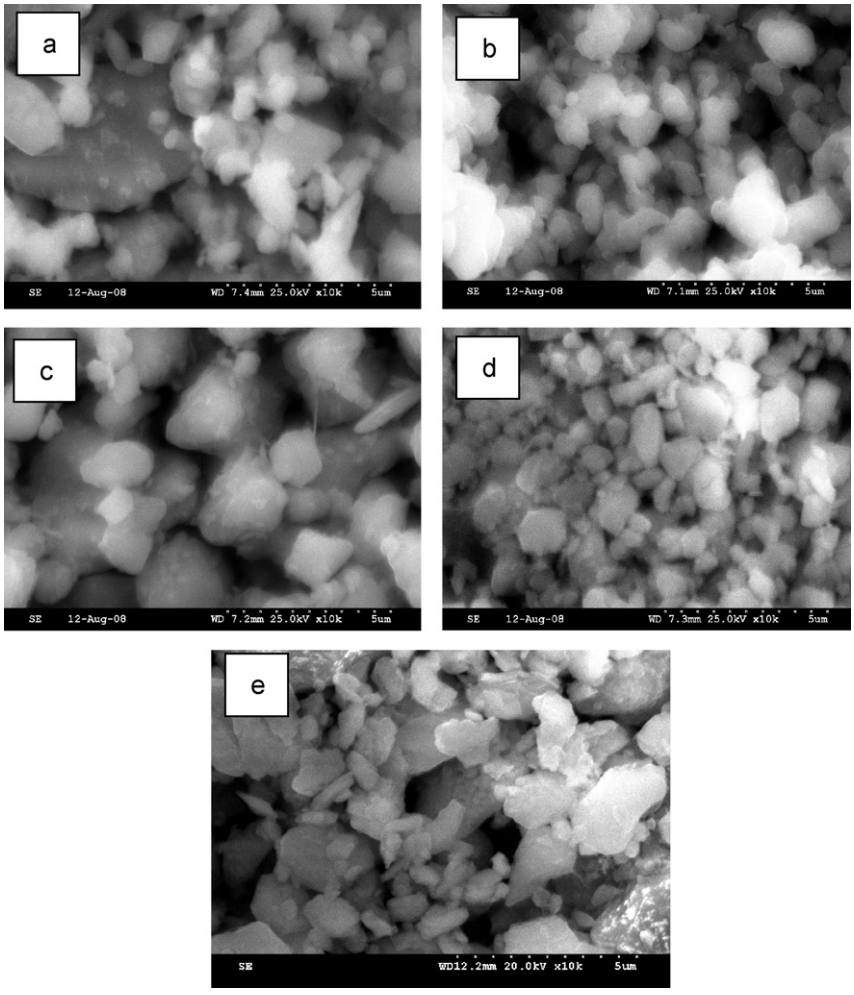

Fig. 3. SEM images of $LiCu_xCo_{1-x}O_{2\pm\delta}$ (a) $x = 0.00$, (b) $x = 0.05$, (c) $x = 0.10$, (d) $x = 0.20$ (e) $x = 0.30$.

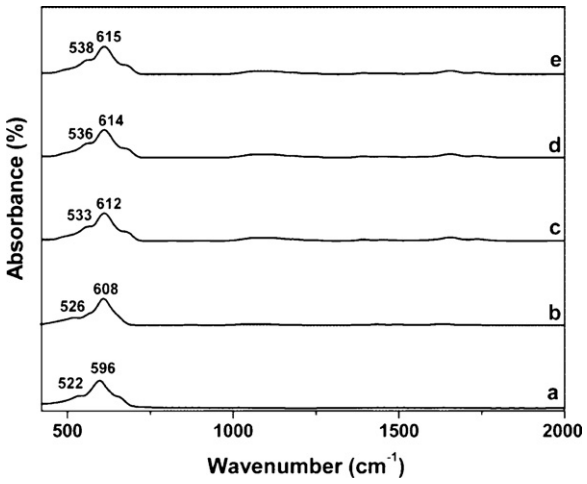

Fig. 4. FT-IR spectra of $LiCu_xCo_{1-x}O_{2\pm\delta}$ (a) $x = 0.00$, (b) $x = 0.05$, (c) $x = 0.10$, (d) $x = 0.20$ (e) $x = 0.30$.

oven and ground well for 2 h to obtain phase pure compound of $LiCu_xCo_{1-x}O_2$.

The synthesized product was characterized by means of XRD ('Xpert PRO PAN alytical PW 3040/60 'X'Pert PRO') using Cu–K_α radiation ($\lambda = 1.5418$ Å), while the voltage and current were held at 40 kV and 20 mA ($2\theta = 0$–80°) at a scan rate of 1° min^{-1}. The surface morphology and microstructure of synthesized samples were characterized by scanning electron microscope (SEM Hitachi S-3000 H from Japan). Fourier Transform Infrared spectrum has been recorded on a Nicolet 5DX-FTIR spectroscopy using KBr pellet in the range of 400–2000 cm^{-1}. X-ray photoelectron spectroscopy (XPS) of synthesized powder has been investigated using VG electron spectroscopy. The powder sample has been pressed into the pellets and affixed on to the sample holder. All spectra were recorded using an X-ray source (Al K_α radiation) with a scan range of 0–1200 eV binding energy. The collected high-resolution XPS spectra were analyzed using XPS peak fitting software program. The energy scale was adjusted using carbon peak, C 1s spectra at 284.5 eV.

The cathode disc has been prepared by mixing 80 wt% active materials, 10 wt% acetylene black and 10 wt% polyvinylidene fluoride (PVDF) binder in N-methylpyrrolidone (NMP) solvent to form homogeneous slurry. The mixture was coated over an aluminium foil and dried under ambient condition and cut into circular discs of 18 mm diameter. The cut discs were further dried under vacuum at 120 °C for 12 h. Finally, 2016 coin type cells have been assembled in an argon filled glove box using lithium as the counter and reference electrode, celgard 2400 as the separator and $LiPF_6$ in 1:1 EC/DEC as the electrolyte solution. The charge/discharge measurements were carried out on the assembled coin cell using a programmable battery tester at 0.1 C (current density around 0.2906 mA cm^{-2}) and 0.2 C (current density around 0.5812 mA cm^{-2}) rates for 50 cycles in the potential range of 2.7–4.6 V.

3. Results and discussion

Fig. 1 shows the XRD patterns of $LiCu_xCo_{1-x}O_{2\pm\delta}$ ($x = 0.00$, 0.05, 0.10, 0.20 and 0.30) samples synthesized using microwave method. As can be seen from Fig. 1, the diffraction patterns are characteristic of the α-$NaFeO_2$ type structure [19] and could be indexed on the basis of $R3m$ space group. Co_3O_4 impurity peaks lying between 2θ values of 34 and 40° (Fig. 2) and also the characteristic peaks of Cu [(1 1 1) and (2 0 0) (JCPDS 03-1005)] at 2θ values of 43.2° and 51° are not identified in the XRD clearly indicating the formation of the single phase compound. The splitting of the diffraction patterns at (0 0 6) (1 0 2) and (1 0 8) (1 1 0) doublets suggests the formation of highly ordered layered structure. The hexagonal parameters of the synthesized material are calculated using the unit cell package software and are presented in Table 1. It can be seen from Table 1 that the 'a' and 'c' values for the synthesized samples are in good agreement with the previous researchers [20]. It can be noted that the ratio of the intensities of (0 0 3) and (1 0 4) peaks i.e., (I_{003}/I_{104}) is greater than unity, thereby suggesting no cation disorder which is supplemented by the values of c/a i.e., > 4.89. According to Dahn et al. [21,22] the R factor [$R = (I_{102} + I_{006})/I_{101}$] is an indicator of hexagonal ordering. We observe that R factor is minimum for $LiCu_{0.2}Co_{0.8}O_{1.9}$ i.e., 0.41, which suggest increased layered characteristics than the pristine $LiCoO_2$ and other copper doped samples. The crystallite sizes are calculated by well known Debye–Scherrer's equation and are found to be very smaller crystallite size of ~100 nm for $LiCu_{0.2}Co_{0.8}O_{1.9}$ as compared to other samples. Scanning electron micrographs of $LiCu_xCo_{1-x}O_{2\pm\delta}$ ($x = 0.00$, 0.05, 0.10, 0.2 and 0.3) samples synthesized by microwave method are shown in Fig. 3 and shows that the particles are agglomerated which decreases with increasing copper content and the smaller particle size obtained for the composition $x = 0.2$ as compared to other samples.

Fig. 4 shows the FTIR spectra of samples $LiCu_xCo_{1-x}O_{2\pm\delta}$ ($x = 0.00$, 0.05, 0.10, 0.20 and 0.30) synthesized by microwave

Table 1
Unit cell parameters of $LiCu_xCo_{1-x}O_{2\pm\delta}$ materials.

x	a (Å)	c (Å)	c/a	Cell volume	I_{003}/I_{004}	R	Crystallite size (nm)
0	2.812	14.014	4.983	96.003	2.49	0.53	150
0.05	2.814	14.039	4.988	96.083	1.74	0.47	132
0.10	2.814	14.055	4.994	96.095	1.60	0.45	125
0.20	2.815	14.068	4.997	96.103	1.49	0.41	100
0.30	2.817	14.081	4.998	96.118	1.42	0.43	120

Table 2
Charge/discharge capacities of $LiCu_xCo_{1-x}O_{2\pm\delta}$ materials.

x	Discharge capacity (mAh g^{-1})					
	0.1 C rate			0.2 C rate		
	1st cycle	50th cycle	Capacity retention (%)	1st cycle	50th cycle	Capacity retention (%)
0	135	85	63	110	70	63
0.05	140	120	86.7	130	100	77
0.10	152	131	87.2	147	126	86.3
0.20	161	143	89.4	153	136	89.1
0.30	159	142	89.3	151	133	88.2

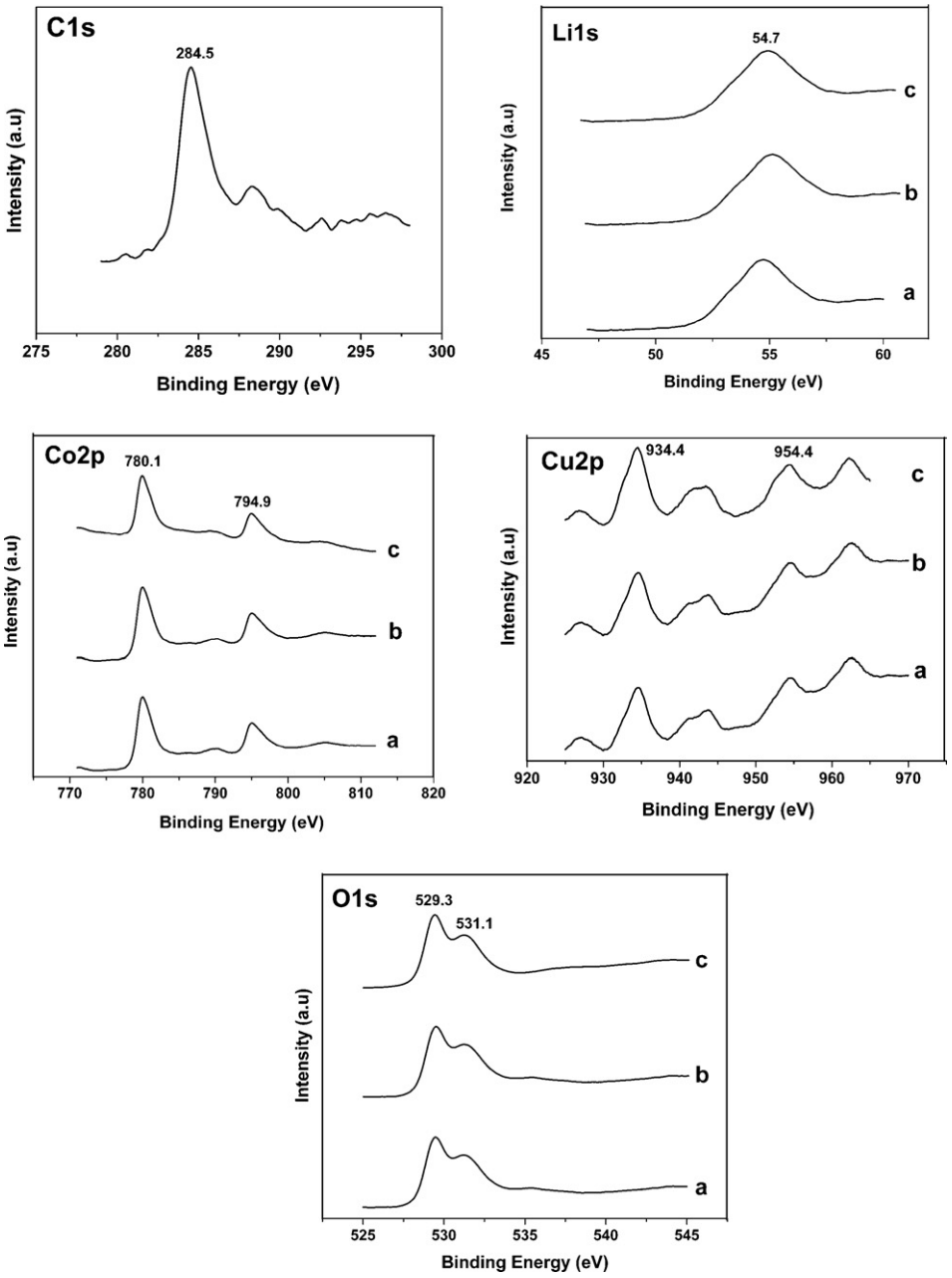

Fig. 5. X-ray photoelectron spectroscopy of $LiCu_xCo_{1-x}O_{2\pm\delta}$ (a) $x = 0.05$, (b) $x = 0.10$, (c) $x = 0.20$.

method scanned in the wave number region 400–2000 cm^{-1}. The band around 529 cm^{-1} has been assigned to Li–O [23] stretching vibration, which indicates the formation of LiO_6 octahedra. The characteristic vibrations of Co–O [24] are 560–590 cm^{-1} and Cu–O [25] is 614 cm^{-1}. The broad absorption band observed at 608 cm^{-1} in copper doped samples may be due to mixed vibration bands of Co–O and Cu–O. The broadening of the high-wavenumber IR bands may be related with inhomogeneous Cu/Co distribution and/or polyhedral distortion occurring in these materials [26].

The oxidation states of Cu and Co are determined from XPS analysis and are depicted in Fig. 5. C 1s emission peak is observed at 284.5 eV, which is used as the reference in the present XPS measurements. Li 1s peak at 54.7 eV, which is the specific arrangement of lithium atoms between the close-packed layers of oxygen in $LiCu_xCo_{1-x}O_{2\pm\delta}$ (octahedral arrangement of oxygen atoms). XPS peak of Co2p corresponds to Co2p → Co3p transitions and is dominated by multiple effects. The Co2p spectrum is split by spin–orbital interaction into $Co2p_{1/2}$ and $Co2p_{3/2}$ regions. In turn these regions are further split due to Co2p–Co3d interaction and crystal field effects. The shapes of the spectra are directly related to the ground state of Co ions [27]. The Co2p bands are observed at 780.1 eV for $Co2p_{3/2}$ and 794.9 eV for $Co2p_{1/2}$. These two bands correspond to Co^{3+} in the synthesized materials. Two peaks are observed, one at 934.4 eV for $Cu2p_{3/2}$, and another one at 954.4 eV for $Cu2p_{1/2}$. The $Cu2p_{3/2}$ and $Cu2p_{1/2}$ main doublets are separated by ~20 eV are seen together with the satellites at ~8 eV from the main peaks. Similar satellite structure was observed in CuO [28], indicating that Cu ions are mostly divalent. O 1s XPS spectra of $LiCu_xCo_{1-x}O_2$ materials are broken down into two components with the main one at 529.3 eV and next at 531.1 eV which are characteristic of O^{2-} ions of the crystalline network. Notwithstanding the attribution of the component on the high-energy side is more difficult, a reasonable hypothesis is to consider, as reported in previous works on cobalt and nickel oxides [29], the existence of defects in the sub-

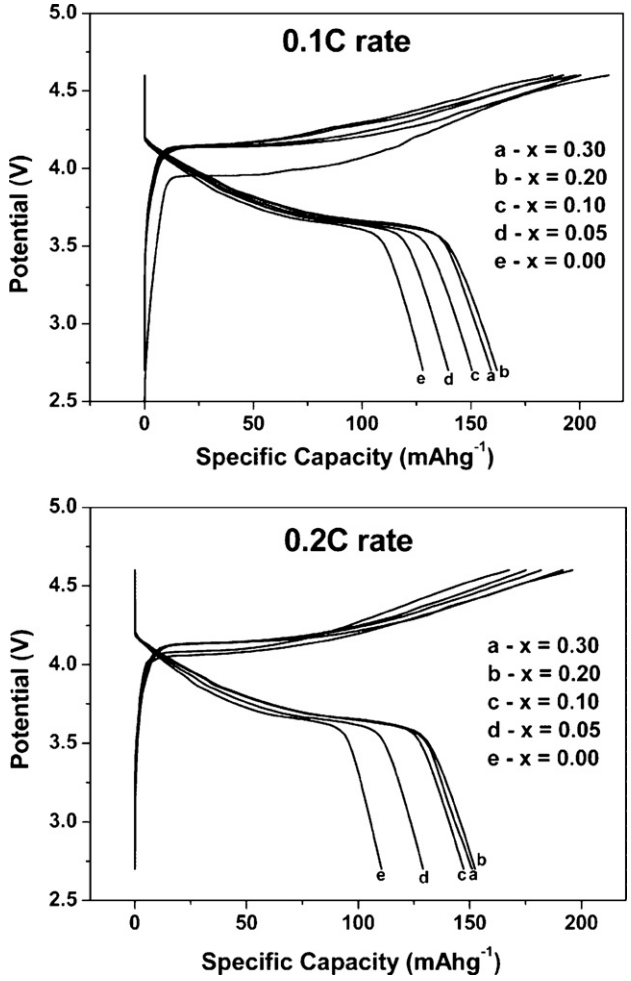

Fig. 6. Charge–discharge behaviour of $LiCu_xCo_{1-x}O_{2\pm\delta}$ at 0.1 and 0.2 C rates.

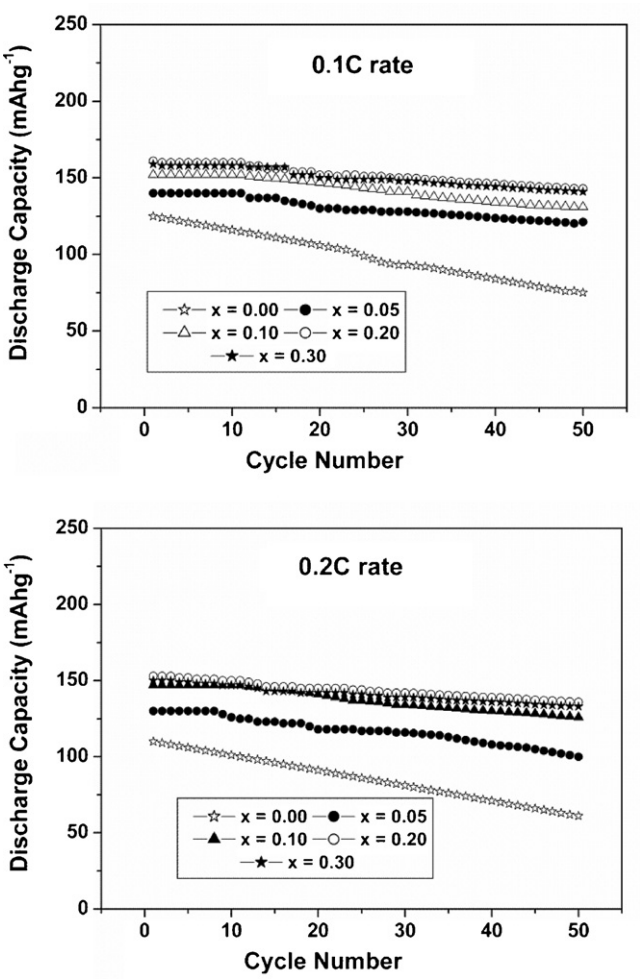

Fig. 7. Cycling performance of $LiCu_xCo_{1-x}O_{2\pm\delta}$ at 0.1 and 0.2 C rates.

surface associated with sites where the coordination number of oxygen ions is smaller in the regular sites. These results are in good agreement with previously reported results [30].

Fig. 6 shows the galvanostatic charge/discharge curves of $LiCu_xCo_{1-x}O_{2\pm\delta}$ measured at 0.1 and 0.2 C rates in the voltage range of 2.7–4.6 V. Table 2 depicts the charge–discharge capacities of undoped and doped $LiCu_xCo_{1-x}O_{2\pm\delta}$ during the 1st and 50th cycle at 0.1, 0.2 C rate with capacity retention. The initial discharge capacities (135, 140, 152, 161 and 159 mAh g^{-1} for $x = 0.00$, 0.05, 0.1, 0.2 and 0.3 at 0.1 C) of the doped materials are higher compared to the undoped $LiCoO_2$. This may be due to the improved structural stability with the addition of dopant, very small volume change and also the collapse of the structure during cycling was prevented by the dopant ion by the limited action of Co^{4+}. The shape of the discharge profiles slightly differs from the pristine $LiCoO_2$ due to oxygen vacancies [31] in the doped materials, hence it could be rewritten as $LiCu_xCo_{1-x}O_{2\pm\delta}$. The discharge capacity of pristine $LiCoO_2$ at the first and 50th cycle is 135 and 85 mAh g^{-1} at 0.1 C rate which is slightly higher than earlier report [32]. Further, at 0.2 C rate, pristine $LiCoO_2$ exhibits 110 and 70 exhibits 110 and 70 mAh g^{-1} for the first and 50th cycle respectively. The poor performance could be ascribed due to the large volume change resulting in structural deterioration during cycling and the synthesis route adopted. In general, the specific capacity decreases at high current rates, which may be attributed to an increase of electrode polarization during cycling as observed by previous researchers [33–35]. Cu doped $LiCoO_2$ materials exhibit the discharge capacities of 120, 131, 143 and 141 mAh g^{-1} at the 50th cycle and discharge capacity fades of 13.3%, 12.8%, 10.6 and 10.7% for the Cu contents corresponding to 0.05, 0.10, 0.20 and 0.30 at C/10. When the copper content increases from 0.2 to 0.3, almost similar discharge capacity and retention in capacity is observed at the end of 50th cycle. Good capacity retention (Fig. 7) has been observed in the present case when compared to other previous researchers [7,16,36,37] and may be due to the dopant Cu^{2+} that may move to the electrode surface and form a solid solution as charge and discharge continues. The solid solution acts as a coating layer and prevents the dissolution of Co^{4+} ions into the electrolyte. This is the first time such a stable high capacities are obtained at high voltage of 4.6 V by doping, albeit Fey et al. proposed that the improved performance obtained through coating (La_2O_3) process at 4.5 V [16]. Cu dopant improves the cycling stability of $LiCoO_2$ material and further as reported by Yan et al. [38] microwave synthesis controls the lithium loss (4%) compared to conventional calcination process (20–30%). Microwave synthesis of $LiCu_{0.2}Co_{0.8}O_{1.9}$ exhibits better cycling performance, less capacity fade compared to convetional synthesis of $LiCu_{0.05}Co_{0.95}O_2$ and other elemental doping cycled up to 4.5 V [5–7,11,16,36–41]. Hence, microwave synthesis without calcination improves the cycling stability of the synthesized materials compared to the material synthesized by calcination assisted microwave process [5].

Fig. 8 shows the dQ/dE vs. potential curves of $LiCu_xCo_{1-x}O_2$ ($x = 0.00$, 0.05, 0.10, 0.20 and 0.30) at 0.1 and 0.2 C rates respectively. It is evident from the figures that the predominant anodic and cathodic peaks are observed around at 4.14 V and 3.67 V sig-

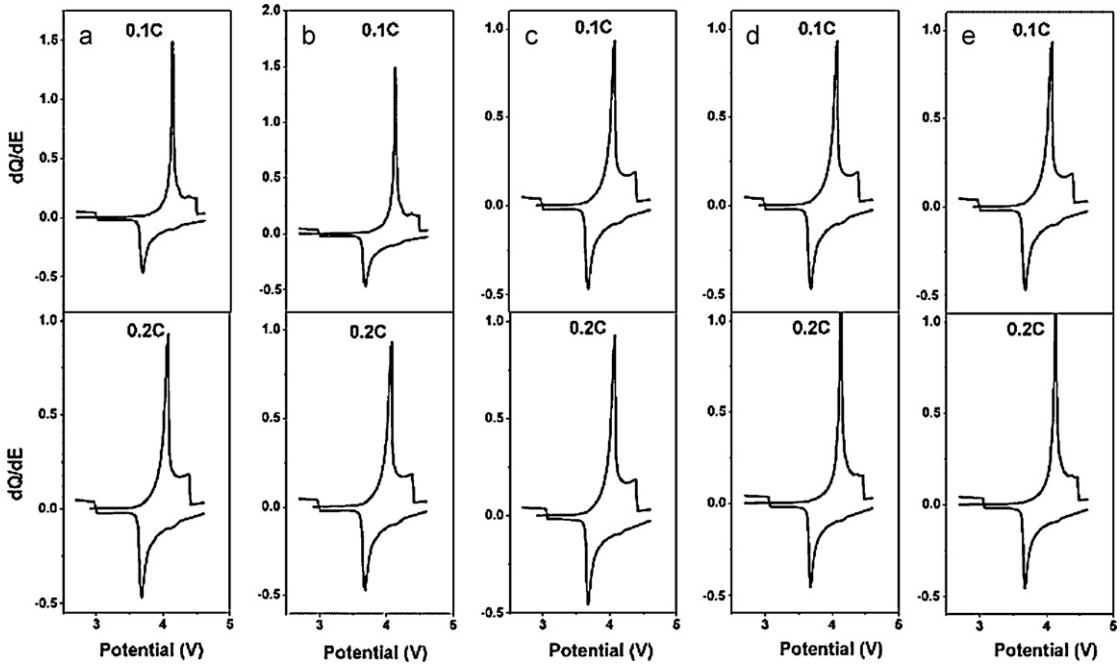

Fig. 8. Differential capacity curves of $LiCu_xCo_{1-x}O_{2\pm\delta}$ (a) $x = 0.00$, (b) $x = 0.05$, (c) $x = 0.10$, (d) $x = 0.20$ (e) $x = 0.30$.

nifying lithium intercalation and deintercalation processes. These peaks are also characteristics of the hexagonal phase in these types of layered compounds [7]. These results suggest that the compounds synthesized by microwave method which are electrochemically active and indicate the charge–discharge process occurs in a reversible manner in the voltage region of 2.7–4.6 V which delivers the high capacity of $\sim$150 mAh g^{-1}.

4. Conclusions

$LiCu_xCo_{1-x}O_{2\pm\delta}$ ($x = 0.00$, 0.05, 0.10, 0.20 and 0.30) cathode materials have been synthesized using microwave method for the first time and $LiCu_{0.2}Co_{0.8}O_{1.9}$ delivers a high capacity of $\sim$150 mAh g^{-1} over the investigated 50 cycles when cycled between 2.7–4.6 V. XRD patterns reveal the high degree of crystallinity without any additional impurity peaks for Cu and Co_3O_4 in the synthesized materials. It is evident to conclude that Cu doped $LiCoO_2$ materials synthesized by this method deliver superior stable capacities at high voltage (4.6 V) over the pristine $LiCoO_2$ cathode materials.

Acknowledgement

The authors thank Council of Scientific Industrial and Research (CSIR) for supporting under the CSIR (India) – Royal Society (UK) project IST01/08.

References

[1] J.B.J. Veldhis, F.C. Eckes, L. Plomp, J. Electrochem. Soc. 39 (1992) L6–8.
[2] L. Plomp, J.B.J. Veldhis, E.F. Slitters, S.B. Van Der Molen, J. Power Sources 39 (1992) 369–373.
[3] K.M. Shaju, G.V. Subba Rao, B.V.R. Chowdari, Electrochim. Acta 48 (2002) 145–151.
[4] S.T. Myung, N. Kumagi, S. Komaba, H.T. Caung, Solid State Ionics 139 (2001) 47–56.
[5] C.N. Zaheena, C. Nithya, R. Thirunakaran, A. Sivashanmugam, S. Gopukumar, Electrochim. Acta 54 (2009) 2877–2882.
[6] H.S. Kim, T.K. Ko, B.K. Na, W.I. Cho, B.W. Chao, J. Power Sources 138 (2004) 232–239.
[7] S. Gopukumar, Y. Jeong, K.B. Kim, Solid State Ionics 159 (2003) 223–232.
[8] S.H. Huang, Z.Y. Wen, X.L. Yang, Z.H. Gu, X.H. Xu, J. Power Sources 148 (2005) 72–77.
[9] J.T. Son, K.S. Park, H.G. Kim, H.T. Chung, J. Power Sources 126 (2004) 182–185.
[10] R. Guo, X. Shi, Y. Cheng, Y. Ma, Z. Tan, J. Power Sources 189 (2002) 2–8.
[11] S. Deepa, N.S. Arvindan, C. Sugadev, R. Tamilselvi, M. Sakthivel, A. Sivashanmugam, S. Gopukumar, Bull. Electrochem. 15 (1999) 381–384.
[12] M. Zou, M. Yoshio, S. Gopukumar, J. Yamaki, Chem. Mater. 15 (2003) 4699–4702.
[13] S.M. Lala, L.A. Montoro, V. Lemos, M. Abbate, J.M. Rosolen, Electrochim. Acta 51 (2005) 7–13.
[14] J. Cho, Y.J. Kim, B. Park, Chem. Mater. 12 (2000) 3788–3791.
[15] J. Cho, Y.J. Kim, B. Park, Angew. Chem. Int. Ed. 40 (2001) 3367–3369.
[16] G.T.K. Fey, P. Muralidharan, C.Z. Lu, Y.D. Cho, Electrochim. Acta 51 (2006) 4850–4858.
[17] H. Zhao, L. Gao, W. Qiu, X. Zhang, J. Power Sources 132 (2004) 195–200.
[18] K.J. Rao, B. Vaidhyanathan, M. Ganguli, P.A. Ramakrishnan, Chem. Mater. 11 (1999) 882–895.
[19] I. Belharouat, W. Lu, D. Vissers, K. Amine, Electrochem. Commun. 8 (2006) 329–335.
[20] I. Saadoune, C. Delmas, J. Solid State Chem. 136 (1998) 8–15.
[21] J.R. Dahn, U. Von Sacken, C.A. Michal, Solid State Ionics 44 (1990) 87–97.
[22] J.N. Reimers, E. Rossen, C.D. Jones, J.R. Dahn, Solid State Ionics 61 (1993) 335–344.
[23] W. Huang, R. Frech, Solid State Ionics 86–88 (1996) 395–400.
[24] Y. Gu, D. Chen, X. Jian, J. Phys. Chem. B 109 (2005) 17901–17906.
[25] A. Sulochana, R. Thirunakaran, A. Sivashanmugam, S. Gopukumar, J. Yamaki, J. Electrochem. Soc. 155 (2008) A206–A210.
[26] M. Nazri, D. Curtis, G.A. Yebka, C. Julien, Extended Abstracts of 193th Meeting of the Electrochem. Soc. 98–1, San Diego, CA, 3–8 May, 1998.
[27] P. Balbuena, Y. Wang (Eds.), Lithium-Ion Batteries: Solid Electrolyte Interphase, Imperial College Press, 2004, p. 185.
[28] G. Fortunato, H.R. Oswald, A. Reller, J. Mater. Chem. 11 (2001) 905–911.
[29] J.C. Dupin, D. Gonbeau, P. Vinatier, A. Levasseur, Phys. Chem. Chem. Phys. 2 (2000) 1319–1324.
[30] V.R. Galakhov, E.Z. Kumrmaev, St. Uhlenbrock, M. Neumann, D.G. Kellerman, V.S. Gorshkov, Solid State Commun. 99 (1996) 221–224.
[31] B. Deng, H. Nakamura, M. Yoshio, J. Power Sources 180 (2008) 864–868.
[32] P. Elumalai, H.N. Vasan, N. Munichandraiah, J. Power Sources 125 (2004) 77–84.
[33] R. Ruffo, C. Wessells, R.A. Huggins, Y. Cui, Electrochem. Commun. 11 (2009) 247–249.
[34] W. Yoon, K.B. Kim, J. Power Sources 81–82 (1999) 517–523.
[35] S.A. Needham, G.X. Wang, H.K. Liu, V.A. Drozd, R.S. Liu, J. Power Sources 174 (2008) 828–831.
[36] C. Julien, M.A. Camcho-Lopez, T. Mohan, S. Chitra, P. Kalyani, S. Gopukumar, Solid State Ionics 135 (2000) 241–248.
[37] H.W. Ha, N.J. Yun, M.H. Kim, M.H. Woo, K. Kim, Electrochim. Acta 51 (2006) 3297–3302.
[38] H. Yan, X. Huang, Z. Lu, H. Huang, R. Xue, L. Chen, J. Power Sources 68 (1997) 530–532.
[39] H. Tukamoto, A.R. West, J. Electrochem. Soc. 144 (1997) 3164–3168.
[40] S. Rodrigues, N. Munichandraiah, A.K. Shukla, J. Power Sources 102 (2001) 322–325.
[41] H. Wook, N.J. Yun, M.H. Kim, M.H. Woo, K. Kim, Electrochim. Acta 51 (2006) 3297–3302.